

# Evaluation for Maximum Hosting Capacity of Distributed Generation Considering Active Network Management

Shunnosuke Ikeda

Keio University, Graduate School of Science and Technology, Kanagawa, Japan

Email: ikeda.shunnosuke@gmail.com

Hiromitsu Ohmori

Keio University, Department of System Design Engineering, Kanagawa, Japan

Email: ohm@sd.keio.ac.jp

**Abstract**—With the increasing penetration of renewable Distributed Generation (DG), it is important to assess the Maximum Hosting Capacity (MHC) in active distribution networks. Active Network Management (ANM) such as coordinated voltage control, reactive power compensation, DG curtailment, DG power factor control, network reconfiguration and demand response can play an important role in increasing the MHC. The MHC evaluation problem considering all the above elements of ANM can be formulated as a mixed integer nonlinear programming model. However, this original nonconvex model cannot guarantee convergence to optimality. This paper proposes the mixed integer second-order cone programming model for evaluating the MHC, by using exact linearization and second-order cone relaxation. The modified IEEE 33-bus test system is used to demonstrate the effectiveness of the proposed model and analyze the effect of each ANM element on the MHC increase. The results show that when considering all the above elements of ANM, the gain of the MHC is greater than 62%.

**Index Terms**—distributed generation, maximum hosting capacity, active network management, mixed integer second-order cone programming

## I. INTRODUCTION

In recent years, renewable Distributed Generation (DG) (e.g., photovoltaic, wind, etc.) has been considered as a promising solution to global energy crisis and serious environmental problems, and significant efforts have been made in many countries to promote the installation of renewable DGs to the electricity networks, especially distribution networks [1].

However, increasing the renewable DG penetration brings various negative effects on the operating of distribution networks such as voltage fluctuation, reverse power flow, network loss increase, etc. Moreover, the power output of renewable DGs is unstable due to intermittency of Renewable Energy Sources (RES). These effects will restrict the DG integration [2]. The

main role of Distribution Network Operator (DNO) is to maintain the efficiency and security of the network. Therefore, it is essential for the DNO to evaluate the Maximum Hosting Capacity (MHC) of renewable DGs which can be accommodated in distribution networks without violating the operational constraints such as current and voltage limits, etc.

The Active Network Management (ANM) is known to be the one of the solution to the operational constraints violation caused by high penetration of renewable DGs. The major ANM schemes include coordinated voltage control of On-Load Tap Changers (OLTC), DG Power Factor Control (PFC), Reactive Power Compensation (RPC), DG curtailment and network reconfiguration (NR) and Demand Response (DR) [3]. Several ANM schemes have been proposed to increase the MHC of DGs [4]-[16]. In [4] and [5], multi-stage and stochastic mathematical model is proposed to determine the optimal sizing, timing and placement of renewable DGs in coordination with energy storage systems and reactive power sources. In [6], a stochastic multi-objective optimization model is proposed to maximize the hosting capacity. In [7], the two-stage adjustable robust optimization is employed to deal with the uncertainties of load demands and DG outputs. In [8], an MHC evaluation method considering the robust optimal operation of OLTCs and static var compensators (SVCs) is proposed. In [9], relaxing radiality constraints, a network reconfiguration scheme is presented to select the best network topology to maximize allowable DG penetration. In [10], a multi-period OPF is proposed to investigate the potential benefits from adopting static and dynamic reconfiguration as options to increase the MHC. In [11], a model based on cost-benefit analysis is proposed to maximize the benefit of the DNO and wind farm owner. In [12], a bi-level programming model for distributed wind generation planning under ANM is proposed. In [13], a multi-period OPF is proposed to investigate the MHC considering energy curtailment, OLTC and power factor control as the ANM.

TABLE I. RECENT RELATED WORKS FOR MAXIMIZING HOSTING CAPACITY OF DGs

Year	Reference	RES	DR	Curtailement	OLTC	RPC	PFC	NR	Formulation
2017	[4], [5]	WT&PV				√	√	√	MINLP
2017	[6]	WT		√			√		MINLP
2017	[14]	WT	√	√			√		NLP
2017	[7]	PV			√	√	√	√	MILP
2016	[8]	PV			√	√			MILP
2016	[9]	unspecified						√	MINLP
2016	[15]	PV	√						MINLP
2015	[16]	WT	√	√		√	√		MINLP
2015	[10]	WT		√	√		√	√	MINLP
2014	[11]	WT		√	√	√	√		NLP
2013	[12]	WT		√	√	√	√		MINLP
2011	[13]	WT		√	√		√		NLP
2018	Ours	PV	√	√	√	√	√	√	MISOCP

Additionally, in [14]-[16], the DR is considered to increase the MHC. To the best of our knowledge, as shown in Table I, no work in the literature considers all the above elements of ANM and analyzes the effect of each ANM element on the MHC increase. Therefore, this paper proposes the evaluation model for the MHC considering all the above elements of ANM. The MHC evaluation problem can be formulated as a Mixed Integer Nonlinear Programming (MINLP) model and can be solved by heuristic or metaheuristic techniques. However, these approaches cannot guarantee optimality and their parameters must be tuned by trial and error. This paper transforms the original nonconvex model into Mixed Integer Second-Order Cone Programming (MISOCP) model by using linearization and second-order cone relaxation. Because of the convexity, the proposed model can guarantee to convergence to optimality and can be solved efficiently with commercial solvers. Furthermore, this paper analyzes the effect of each ANM element on the increase of MHC, by using our proposed model.

## II. PROBLEM FORMULATION

The aim of the optimization problem is to evaluate the MHC of DG that can be accommodated by the distribution networks. This section formulates the MHC evaluation problem considering ANM. Using the network model (DistFlow equations) first introduced in [17], the optimization problem is formulated as a MINLP problem. Moreover, by introducing two new variables  $I_{ij,t}^{sqr} = I_{ij,t}^2$  and  $V_{i,t}^{sqr} = V_{i,t}^2$  which respectively represent the square of current and voltage magnitude, the problem can be modeled as follows.

(MINLP model)

$$\max \sum_{i \in \Omega_{dg}} P_i^{dg,cap} \quad (1)$$

subject to switch status constraints:  $\forall j \in N(i), \forall i \in \Omega_{bus}, t \in \Omega_T$

$$u_{ij,t} = u_{ji,t} \quad (2)$$

where  $\Omega_{dg}$  is the sets of candidate buses for DG installation, and  $P_i^{dg,cap}$  is the active power capacity of DG in bus  $i$ .

$$u_{ij,t} \in \{0,1\} \quad (3)$$

where  $\Omega_{bus}$  is the set of buses (i.e.,  $\Omega_{bus} = \{0, \dots, |\Omega_{bus}|\}$ ), and  $N(i)$  is the set of buses connected to bus  $i$ , and  $\Omega_T$  is the set of operating time, and  $u_{ij,t}$  is a binary variable which represent the switch status: equals 1 if branch  $(i,j)$  is connected; otherwise equals 0.

Power balance constraints  $\forall j \in \Omega_{bus}, t \in \Omega_T$

$$\sum_{i \in N(j)} \left( u_{ij,t} P_{ij,t} - \frac{1}{2} r_{ij} u_{ij,t} I_{ij,t}^{sqr} \right) + P_{j,t} = 0 \quad (4)$$

$$\sum_{i \in N(j)} \left( u_{ij,t} Q_{ij,t} - \frac{1}{2} x_{ij} u_{ij,t} I_{ij,t}^{sqr} \right) + Q_{j,t} = 0 \quad (5)$$

$$P_{ij,t}^2 + Q_{ij,t}^2 = V_{i,t}^{sqr} I_{ij,t}^{sqr}, \quad \forall i \in N(j) \quad (6)$$

$$P_{ij,t} = -P_{ji,t}, Q_{ij,t} = -Q_{ji,t}, I_{ij,t}^{sqr} = I_{ji,t}^{sqr}, \quad \forall i \in N(j) \quad (7)$$

where  $P_{ij,t}$  and  $Q_{ij,t}$  are active and reactive power flowing from bus  $i$  to bus  $j$  at time  $t$ , respectively,  $P_{j,t}$  and  $Q_{j,t}$  are active and reactive power injection onto bus  $j$  at time  $t$ , respectively, and  $r_{ij}$  and  $x_{ij}$  are resistance and reactance from bus  $i$  to bus  $j$  at time  $t$ , respectively. Note that  $r_{ij} = r_{ji}$  and  $x_{ij} = x_{ji}$ . Illusive power flows are shown in Fig. 1.

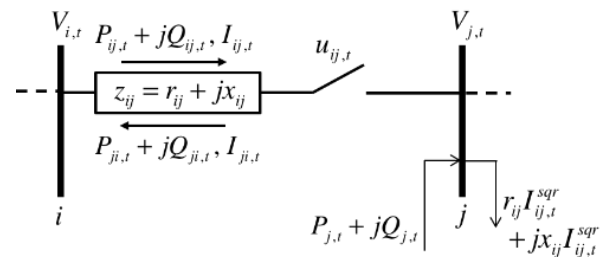


Figure 1. Illusive power flows with two nodes.

Power injection constraints  $\forall j \in \Omega_{bus}, t \in \Omega_T$

$$P_{i,t} = P_{i,t}^{ss} + P_{i,t}^{dg} - P_{i,t}^d - P_{i,t}^{cur} \quad (8)$$

$$Q_{i,t} = Q_{i,t}^{ss} + Q_{i,t}^{dg} - Q_{i,t}^d + Q_{i,t}^{svc} \quad (9)$$

where  $P_{i,t}^{ss}$  and  $Q_{i,t}^{ss}$  are active and reactive power injected from substation onto bus  $i$  across the OLTC at time  $t$ , respectively, and  $P_{i,t}^{dg}$  and  $Q_{i,t}^{dg}$  are active and reactive power outputs of DGs in bus  $i$  at time  $t$ , respectively, and  $P_{i,t}^d$  and  $Q_{i,t}^d$  are active and reactive power demand in bus  $i$  in the presence of DR at time  $t$ , respectively, and  $P_{i,t}^{cur}$  is the curtailed active power of DGs in bus  $i$  at time  $t$ , and  $Q_{i,t}^{svc}$  is reactive power output of SVC in bus  $i$  at time  $t$ .

*Branch equation constraints*  $\forall j \in N(i), \forall i \in \Omega_{bus}, t \in \Omega_T$

$$V_{i,t}^{sqr} - V_{j,t}^{sqr} = 2(r_{ij}u_{ij,t}P_{ij,t} + x_{ij}u_{ij,t}Q_{ij,t}) - z_{ij}^2 I_{ij,t}^{sqr} \quad (10)$$

where  $z_{ij} = r_{ij} + jx_{ij}$  is the impedance from bus  $i$  to bus  $j$ . These constraints can be derived from Ohm's law.

*Voltage constraints*  $\forall j \in \Omega_{bus}, t \in \Omega_T$

$$(V^{min})^2 \leq V_{i,t}^{sqr} \leq (V^{max})^2 \quad (11)$$

where  $V^{min}$  and  $V^{max}$  are minimum and maximum voltage magnitude, respectively.

*Current constraints*

$$0 \leq I_{i,t}^{sqr} \leq (I^{max})^2 \quad (12)$$

where  $I^{max}$  is the maximum current magnitude.

*OLTC constraints of transformer*

$$V_{0,t}^{sqr} = (\gamma_t^{tap})^2 (V^{ss})^2 \quad (13)$$

$$\gamma_t^{tap} = \gamma^{tap,min} + \delta_t^{tap} \Delta\gamma \quad (14)$$

$$0 \leq \delta_t^{tap} \leq \delta^{tap,max} \quad (15)$$

$$\Delta\gamma = (\gamma^{tap,max} - \gamma^{tap,min}) / \delta^{tap,max} \quad (16)$$

$$\delta_t^{tap} \in \{\text{integer}\} \quad (17)$$

where  $V^{ss}$  is a constant representing the substation voltage, and  $\gamma_t^{tap}$  is the turns ratio of the transformer at time  $t$ , and  $\gamma^{tap,min}$  and  $\gamma^{tap,max}$  are minimum and maximum turns ratios of the transformer, and  $\delta_t^{tap}$  is an integer variable that represents the actual tap position of the tap changer at time  $t$ , and  $\delta^{tap,max}$  is the total number of taps of the OLTC [18, 19].

*DG operation constraints*  $\forall i \in \Omega_{dg}, t \in \Omega_T$

$$P_{i,t}^{dg} = w_t^{dg} P_i^{dg,cap} \quad (18)$$

$$-P_{i,t}^{dg} \tan(\cos^{-1}(\theta^{ld})) \leq Q_{i,t}^{dg} \leq P_{i,t}^{dg} \tan(\cos^{-1}(\theta^{lag})) \quad (19)$$

where  $w_t^{dg} \in [0:1]$  is the scalar which represents the generation level of DGs at time  $t$  relative to the DG capacity, and  $\theta^{ld}$  and  $\theta^{lag}$  are the angle of leading and lagging power factor, respectively.

*Curtailed energy constraints*  $\forall i \in \Omega_{dg}, t \in \Omega_T$

$$0 \leq P_{i,t}^{cur} \leq P_{i,t}^{dg} \quad (20)$$

$$\sum_{t \in \Omega_T} P_{i,t}^{cur} \Delta t \leq \alpha^{cur} \sum_{t \in \Omega_T} P_{i,t}^{dg} \Delta t \quad (21)$$

where  $\Delta t$  is the time duration of each time interval and  $\alpha^{cur}$  is the maximum percentage of allowed energy curtailment.

*Load shifting constraints of DR*  $\forall i \in \Omega_d, t \in \Omega_T$

$$\bar{P}_{i,t}^d (1 - \beta^{dr,min}) \leq P_{i,t}^d \leq \bar{P}_{i,t}^d (1 + \beta^{dr,max}) \quad (22)$$

$$\bar{Q}_{i,t}^d (1 - \beta^{dr,min}) \leq Q_{i,t}^d \leq \bar{Q}_{i,t}^d (1 + \beta^{dr,max}) \quad (23)$$

$$\sum_{t \in \Omega_T} P_{i,t}^d \Delta t = \sum_{t \in \Omega_T} \bar{P}_{i,t}^d \Delta t \quad (24)$$

$$\sum_{t \in \Omega_T} Q_{i,t}^d \Delta t = \sum_{t \in \Omega_T} \bar{Q}_{i,t}^d \Delta t \quad (25)$$

where  $\Omega_d$  is the set of demand buses, and  $\bar{P}_{i,t}^d$  and  $\bar{Q}_{i,t}^d$  are original active and reactive power demand before DR participation in bus  $i$  at time  $t$ , respectively, and  $\beta^{dr,min}$  and  $\beta^{dr,max}$  are minimum and maximum limit of DR.

*Network radiality constraints*  $t \in \Omega_T$

$$\sum_{(i,j) \in \Phi_{br}} u_{ij,t} = |\Omega_d| - |\Omega_{ss}| \quad (26)$$

$$u_{ij} = 1, \quad \forall j \in N(i), \forall i \in \Omega_{ss} \quad (27)$$

$$v_{ij,t} \in \{0,1\}, \quad \forall j \in N(i), \forall i \in \Omega_{bus} \quad (28)$$

$$v_{ij,t} + v_{ji,t} = u_{ij,t}, \quad \forall j \in N(i), \forall i \in \Omega_{bus} \quad (29)$$

$$\sum_{j \in N(i)} v_{ij,t} = 1, \quad \forall i \in \Omega_{bus} \setminus \{0\} \quad (30)$$

$$v_{0j,t} = 0, \quad \forall j \in N(0) \quad (31)$$

where  $\Phi_{br}$  is the set of branches. Note that the branch  $(i,j)$  and  $(j,i)$  are not distinguished. Only (26) and (27) cannot ensure the radiality of the network. Thus, it is necessary to consider additional conditions, which are sufficient to guarantee network radiality. Here, introducing two binary variables  $v_{ij,t}, v_{ji,t}$ , such additional conditions (28)-(31) are added. Equation (29) shows that a branch  $(i,j)$  is in the spanning tree ( $u_{ij,t} = 1$ ) if either bus  $j$  is the parent of bus  $i$  ( $v_{ij,t} = 1$ ), or bus  $i$  is the parent of bus  $j$  ( $v_{ji,t} = 1$ ). Equation (30) means that all buses except the substation have only one parent. Also, (31) indicates that the substation bus has no parents. When (26)-(31) are satisfied, it is guaranteed that distribution network corresponds to a spanning tree connected to the substation, regardless of the direction of power flow [20].

*Reactive power constraints of SVC*  $\forall i \in \Omega_{svc}, t \in \Omega_T$

$$-Q_i^{svc,cap} \leq Q_{i,t}^{svc} \leq Q_i^{svc,cap} \quad (32)$$

where  $\Omega_{svc}$  is the set of buses at which SVCs have been installed, and  $Q_i^{svc,cap}$  is the reactive power capacity of SVC in bus  $i$ .

In this model, the decision variables are as follows:  
Continuous variables:

$$P_{ij,t}, Q_{ij,t}, P_{i,t}, Q_{i,t}, P_{i,t}^{ss}, Q_{i,t}^{ss}, P_{i,t}^{dg}, Q_{i,t}^{dg}, P_{i,t}^d, Q_{i,t}^d, P_{i,t}^{cur}, Q_{i,t}^{svc}, P_i^{dg,cap}, I_{ij,t}^{sqr}, V_{i,t}^{sqr}, \gamma_t^{tap}.$$

Integer variable is  $\delta_t$  and Binary variable is  $u_{ij,t}$ .

### III. PROPOSED OPTIMIZATION MODEL

The formulation of the MHC evaluation problem represented by (1)-(32) is a nonconvex MINLP model. However, due to its nonconvexity ((4)-(6), (10), (13) and (14)), it is hard to solve this problem or guarantee the convergence to optimality. This paper introduces convexification of these nonconvex constraints and changes the original nonconvex model into MISOCP model.

#### A. Linearization of Bilinear Constraints

In this subsection, nonconvex constraints (4), (5) and (10) are linearized. These constraints are nonconvex due to the presence of the bilinear terms  $u_{ij,t}P_{ij,t}$ ,  $u_{ij,t}Q_{ij,t}$  and  $u_{ij,t}I_{ij,t}^{sqr}$ . In order to linearize them, the disjunctive constraints are used as follows [19]:  $\forall i \in \Omega_{bus}, \forall j \in N(i), t \in \Omega_T$

$$-u_{ij,t} \cdot S^{max} \leq P_{ij,t} \leq u_{ij,t} \cdot S^{max} \quad (33)$$

$$-u_{ij,t} \cdot S^{max} \leq Q_{ij,t} \leq u_{ij,t} \cdot S^{max} \quad (34)$$

$$0 \leq I_{ij,t}^{sqr} \leq u_{ij,t} \cdot (I^{max})^2 \quad (35)$$

where  $S^{max}$  is maximum apparent power. By introducing (33)-(35),  $u_{ij,t}P_{ij,t}$ ,  $u_{ij,t}Q_{ij,t}$  and  $u_{ij,t}I_{ij,t}^{sqr}$  can be replaced by  $P_{ij,t}$ ,  $Q_{ij,t}$  and  $I_{ij,t}^{sqr}$ , respectively. Therefore, the power balance constraints ((4) and (5)) and the part of branch equation constraints (10) can be rewritten as follows:  $\forall j \in \Omega_{bus}, t \in \Omega_T$

$$\sum_{i \in N(j)} \left( P_{ij,t} - \frac{1}{2} r_{ij} I_{ij,t}^{sqr} \right) + P_{j,t} = 0 \quad (36)$$

$$\sum_{i \in N(j)} \left( Q_{ij,t} - \frac{1}{2} x_{ij} I_{ij,t}^{sqr} \right) + Q_{j,t} = 0 \quad (37)$$

$$V_{i,t}^{sqr} - V_{j,t}^{sqr} \leq (1 - u_{ij,t})((V^{max})^2 - (V^{min})^2) + 2(r_{ij}P_{ij,t} + x_{ij}Q_{ij,t}) - z_{ij}^2 I_{ij,t}^{sqr}, \quad \forall i \in N(j) \quad (38)$$

$$V_{i,t}^{sqr} - V_{j,t}^{sqr} \geq -(1 - u_{ij,t})((V^{max})^2 - (V^{min})^2) + 2(r_{ij}P_{ij,t} + x_{ij}Q_{ij,t}) - z_{ij}^2 I_{ij,t}^{sqr}, \quad \forall i \in N(j) \quad (39)$$

After the above transformation, the remaining nonconvex constraints in the original MINLP model are (6) and (13).

#### B. Linearization of OLTC Constraints

This subsection linearizes the nonconvex constraints (13). These constraints are nonconvex due to the presence of the square of the variable  $(\gamma_t^{tap})^2$ . In order to linearize it, (14) are rewritten by the binary expansion scheme as follows:  $t \in \Omega_T$

$$\gamma_t^{tap} = \gamma^{tap,min} + \Delta\gamma \sum_{n=0}^L 2^n \lambda_{n,t}^{tap} \quad (40)$$

$$\sum_{n=0}^L 2^n \lambda_{n,t}^{tap} \leq \delta^{tap,max} \quad (41)$$

$$\lambda_{n,t}^{tap} \in \{0,1\}, \quad \forall n \in \{0, \dots, L\} \quad (42)$$

where  $\lambda_{n,t}^{tap}$  is a binary variable and L is the length of the binary expression of  $\delta^{tap,max}$ . Multiplying both sides of (40) by  $(V^{ss})^2$  and defining new variables  $\mu_{n,t}^{tap} = \lambda_{n,t}^{tap} \gamma_{n,t}^{tap}$ , (40) can be represented as follows:  $t \in \Omega_T$

$$V_{0,t}^{sqr} = (V^{ss})^2 \gamma^{tap,min} \gamma_t^{tap} + (V^{ss})^2 \Delta\gamma \sum_{n \in \Omega_{tap}} 2^n \mu_{n,t}^{tap} \quad (43)$$

Here, introducing a positive large number M,  $\mu_{n,t}^{tap} = \lambda_{n,t}^{tap} \gamma_{n,t}^{tap}$  can be equivalently replaced as follows [18]:  $t \in \Omega_T, \forall n \in \{0, \dots, L\}$

$$0 \leq \gamma_t^{tap} - \mu_{n,t}^{tap} \leq (1 - \lambda_{n,t}^{tap})M \quad (44)$$

$$0 \leq \mu_{n,t}^{tap} \leq \lambda_{n,t}^{tap} M \quad (45)$$

By performing the above transformation, the nonconvex constraint (13) can be replaced by mixed integer linear constraints (40)-(42) and (43)-(45).

#### C. Second-order cone relaxation

In this subsection, nonconvex equality constraints (6) are transformed into the second-order cone constraints shown in the following equations [21]:  $\forall j \in N(i), \forall i \in \Omega_{bus}, t \in \Omega_T$

$$P_{ij,t}^2 + Q_{ij,t}^2 \leq V_{i,t}^{sqr} I_{ij,t}^{sqr} \quad (46)$$

The relaxed constraints (46) can be written as the following convex second-order cone constraints.

$$\left\| \begin{array}{c} 2P_{ij,t} \\ 2Q_{ij,t} \\ I_{ij,t}^{sqr} - V_{i,t}^{sqr} \end{array} \right\|_2 \leq I_{ij,t}^{sqr} + V_{i,t}^{sqr} \quad (47)$$

#### D. MISOCP Model for MHC

After the above transformation such as linearization and second-order cone relaxation (3.1-3.3), the MINLP model for MHC given by objective function and constraints (1)-(32) becomes the following MISOCP model.

(MISOCP model)

$$\max \sum_{i \in \Omega_{dg}} P_i^{dg,cap} \quad (48)$$

subject to

- Current constraints given by (35)
- OLTC constraints of transformer given by (16), (40)-(42), (43)-(45)
- DG operation constraints given by (18) and (19)
- Curtailed energy constraints of DGs given by (20) and (21)
- Power injection constraints given by (8) and (9)
- Branch equation constraints given by (38) and (39)
- Voltage constraints given by (35)

- Power balance constraints given by (7), (33), (34), (36), (37) and (47)
- Switch status constraints given by (2) and (3)
- Load shifting constraints of DR given by (22)-(25)
- Network radiality constraints given by (26)-(31)
- Reactive power constraints of SVC given by (32)

In this model, the decision variables are as follows:  
Continuous variables:

$$P_{ij,t}, Q_{ij,t}, P_{i,t}, Q_{i,t}, P_{i,t}^{ss}, Q_{i,t}^{ss}, P_{i,t}^{dg}, Q_{i,t}^{dg}, P_{i,t}^d, Q_{i,t}^d, P_{i,t}^{cur}, Q_{i,t}^{svc}, P_{i,t}^{dg,cap}, I_{ij,t}^{sqr}, V_{i,t}^{sqr}, \gamma_t^{tap}, \mu_{n,t}^{tap}.$$

Binary variables:  $u_{ij,t}, \lambda_{n,t}^{tap}$ .

#### IV. NUMERICAL SIMULATION

The modified IEEE 33-bus test system from [22] is selected for our numerical simulations. The proposed optimization model was solved using the commercial solver Gurobi Optimizer 7.5.2 on a computer with a 2.3 GHz Intel core i7 processor and 256GB of RAM.

##### A. Test System

As shown in Fig. 2, the modified IEEE 33-bus test system is radial distribution network with one substation, which has 33 buses, 37 branches, 32 sectionalizing switches, 5 tie switches. The voltage of substation ( $V^{SS}$ ) is 12.66kV and the peak load is 3.175MW and 2.3MVar. In this simulation, candidate buses for DG installation are bus 5, bus 10, bus 15, bus 21, bus 24, bus 27 and bus 30, and photovoltaics (PV) are chosen as a type of DGs. Also, buses at which SVCs have been installed are bus 17 and bus 32. The time segment are assigned intervals of 1 hour for a 24 hour periods. The other simulation parameters are shown in Table II.

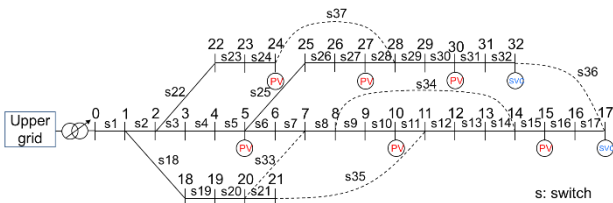


Figure 2. Modified IEEE 33-bus test system.

TABLE II. SIMULATION PARAMETERS

Current limit $I^{max}$	300A
Voltage limit $V^{min}, V^{max}$	0.95 p.u. ~ 1.05 p.u.
Apparent power limit $S^{max}, S^{ss,max}$	6.6MW
Turn ratio limit of OLTC $\gamma^{tap,min}, \gamma^{tap,max}$	0.95, 1.05
Number of total taps of OLTC $\delta^{tap,max}$	10
Leading power factor $\cos(\theta^{ld})$	0.95
Lagging power factor $\cos(\theta^{lag})$	0.95
Curtailement limit $a^{cur}$	10%
DR limit $\beta^{dr,min}, \beta^{dr,max}$	10%
SVC capacity $Q^{svc,cap}$	500kVar

##### B. Load and DG Profile

In this paper, the worst case of demand loads and DG outputs is used when determining the MHC of DGs. This corresponds to the maximum DG outputs at the minimum load levels. As shown in Fig. 3, the minimum load at each time is used from the yearly actual load data of Japan, which are published by the Tokyo Electric Power Company (TEPCO) [23]. The peak load level of the IEEE 33-bus system is used. Also, the PV generation rate is calculated by using yearly actual solar radiation and temperature data collected in Tokyo [24] and the maximum PV output at each time is used as shown in Fig. 4. The data is collected from January 1, 2014 to December 31, 2014.

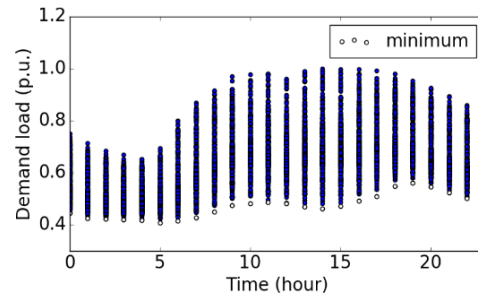


Figure 3. Daily load profile.

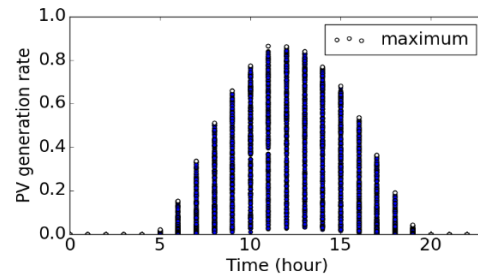


Figure 4. Daily PV output profile.

##### C. Results and Analysis

In this simulation, the following three cases are considered:

Case 1: Only two sites are available for PVs (bus 21 and bus 24).

Case 2: Only four sites are available for PVs (bus 5, bus 15, bus 27 and bus 30).

Case 3: All seven sites are available for PVs (bus 5, bus 10, bus 15, bus 21, bus 24, bus 27 and bus 30).

In addition, the following two cases are also considered.

Case A: ANM schemes are not used (i.e., passive network management).

Case B: All elements of ANM are used.

Table III shows the MHC and compare three PV siting cases.

As the number of buses to install PVs increases, it can be seen in Case A that the MHC increases. On the other hand, in Case B, the MHC is almost the same regardless of the number of PV installation buses.

TABLE III. MHC COMPARISON BY EACH SCHEME

Case	Characteristic	Not Considered (Case A)	Only DR	Only Curtailment	Only OLTC	Only RPC	Only PFC	Only NR	All Considered (Case B)
Case1	MHC (MW)	5.890	6.051	7.558	5.980	6.300	6.372	7.460	10.77
	Gain (%)	-	2.733	28.32	1.528	7.961	8.183	26.65	83.01
Case2	MHC (MW)	6.469	6.733	8.293	6.566	7.060	7.263	7.460	10.77
	Gain (%)	-	4.081	28.20	1.499	9.136	12.27	15.32	66.53
Case3	MHC (MW)	6.696	7.003	8.582	6.845	7.428	7.767	7.460	10.91
	Gain (%)	-	4.584	28.17	2.223	10.93	15.99	11.39	62.93

Moreover, the DR, RPC and DG power factor control show that the gain of the MHC is greater as the number of buses PV installed increase. For these elements, reactive power can be adjusted. Therefore, as the number of PV installation buses increase, it can be considered that the reactive power control becomes more significant for a MHC increase.

From Case1 to Case 3, the PV power Curtailment has the greatest gain of the MHC among each element. However, the gain does not change so much even if the number of PV installation buses increases.

Also, the OLTC has the smallest contribution to the MHC increase in all cases. This is because it is located in the substation bus and only the voltage of the leaf node can be adjusted in the radial network, even if the network reconfiguration is considered. If the OLTC is set to other buses such as ones near PVs, it may be possible to induce greater MHC increase.

When only the network reconfiguration is considered as ANM schemes, it is seen that the same MHC is achieved regardless of the number of installed PVs. In other words, as the number of PV buses gets smaller, the network reconfiguration affects the MHC increase, therefore, it is a very effective means to increase the MHC if the number of PV installed buses is small.

## V. CONCLUSIONS AND FUTURE WORKS

This paper proposed the evaluation model for the MHC considering ANM schemes. The ANM schemes include coordinated voltage control of OLTC, RPC, DG curtailment, DG PFC, NR and DR. The original nonconvex model is converted to a MISOCP model by using linearization and second-order cone relaxation. Because of the convexity, the proposed model can guarantee convergence to optimality and can be solved efficiently with commercial solvers.

The modified IEEE 33-bus test system was used to demonstrate the effectiveness and capability of the proposed model. When considering ANM schemes, the gain of the MHC is greater than 62% in all cases. In addition, from the obtained results, the effect of each ANM factor on the MHC increase was also analyzed.

In this paper, the MHC was evaluated under the worst case without considering the uncertainty of demand and PV outputs. However, the possibility of occurrence of the worst case is very low. Therefore, we hope to evaluate the MHC considering the uncertainty in our future work.

## ACKNOWLEDGMENT

This work was supported by JST CREST Grant Number JPMJCR15K5, Japan.

## REFERENCES

- [1] S. Liew and G. Strbac, "Maximising penetration of wind generation in existing distribution networks," *IEEE Proceedings-Generation, Transmission and Distribution*, vol. 149, no. 3, pp. 256–262, 2002.
- [2] H. Xing and X. Sun, "Distributed generation locating and sizing in active distribution network considering network reconfiguration," *IEEE Access*, vol. 5, pp. 14768–14774, 2017.
- [3] S. S. Al Kaabi, H. Zeineldin, and V. Khadkikar, "Planning active distribution networks considering multi-dg configurations," *IEEE Trans. on Power Systems*, vol. 29, no. 2, pp. 785–793, 2014.
- [4] S. F. Santos, D. Z. Fitiwi, M. Shafie-Khah, A. W. Bizuayehu, C. M. Cabrita, and J. P. Catalao, "New multistage and stochastic mathematical model for maximizing res hosting capacity—part I: problem formulation," *IEEE Trans. on Sustainable Energy*, vol. 8, no. 1, pp. 304–319, 2017.
- [5] S. F. Santos, D. Z. Fitiwi, M. Shafie-khah, A. W. Bizuayehu, C. M. Cabrita, and J. P. Catalao, "New multi-stage and stochastic mathematical model for maximizing res hosting capacity—Part II: Numerical results," *IEEE Trans. on Sustainable Energy*, vol. 8, no. 1, pp. 320–330, 2017.
- [6] A. Rabiee and S. M. Mohseni-Bonab, "Maximizing hosting capacity of renewable energy sources in distribution networks: A multi-objective and scenario-based approach," *Energy*, vol. 120, pp. 417–430, 2017.
- [7] X. Chen, W. Wu, and B. Zhang, "Robust capacity assessment of distributed generation in unbalanced distribution networks incorporating ANM techniques," *IEEE Trans. on Sustainable Energy*, 2017.
- [8] S. Wang, S. Chen, L. Ge, and L. Wu, "Distributed generation hosting capacity evaluation for distribution systems considering the robust optimal operation of OLTC and SVC," *IEEE Trans. on Sustainable Energy*, vol. 7, no. 3, pp. 1111–1123, 2016.
- [9] M. Davoudi, V. Cecchi, and J. R. Aguero, "Network reconfiguration with relaxed radiality constraint for increased hosting capacity of distribution systems," in *Proc. Power and Energy Society General Meeting*, 2016, pp. 1–5.
- [10] F. Capitanescu, L. F. Ochoa, H. Margossian, and N. D. Hatziargyriou, "Assessing the potential of network reconfiguration to improve distributed generation hosting capacity in active distribution systems," *IEEE Trans. on Power Systems*, vol. 30, no. 1, pp. 346–356, 2015.
- [11] S. Nursebo, P. Chen, O. Carlson, and L. B. Tjernberg, "Optimizing wind power hosting capacity of distribution systems using cost benefit analysis," *IEEE Trans. on Power Delivery*, vol. 29, no. 3, pp. 1436–1445, 2014.
- [12] J. Zhang, H. Fan, W. Tang, M. Wang, H. Cheng, and L. Yao, "Planning for distributed wind generation under active management mode," *Int. Journal of Electrical Power & Energy Systems*, vol. 47, pp. 140–146, 2013.
- [13] S. N. Salih, P. Chen, O. Carlson, and N. Shemsedin, "Maximizing wind power integration in distribution system," in *Proc. 10th Int. Workshop Large-Scale Integr. Wind Power Power Syst. Transm. Netw. Offshore Wind Power Plants*, 2011, pp. 625–628.

- [14] A. Soroudi, A. Rabiee, and A. Keane, "Distribution networks' energy losses versus hosting capacity of wind power in the presence of demand flexibility," *Renewable Energy*, vol. 102, pp. 316–325, 2017.
- [15] M. M. Rahman, A. Arefi, G. Shafiullah, and S. Hettiwatte, "Penetration maximisation of residential rooftop photovoltaic using demand response," in *Proc. Int. Conf. on Smart Green Technology in Electrical and Information Systems*, 2016, pp. 21–26.
- [16] A. Soroudi, A. Rabiee, and A. Keane, "Distribution network hosting capacity maximization using demand response," *CIRE2015, June15G18*, 2015.
- [17] M. Baran and F. F. Wu, "Optimal sizing of capacitors placed on a radial distribution system," *IEEE Trans. on power Delivery*, vol. 4, no. 1, pp. 735–743, 1989.
- [18] W. Wu, Z. Tian, and B. Zhang, "An exact linearization method for oltc of transformer in branch flow model," *IEEE Trans. on Power Systems*, vol. 32, no. 3, pp. 2475–2476, 2017.
- [19] Z. Tian, W. Wu, B. Zhang, and A. Bose, "Mixed-integer second-order cone programming model for VAR optimisation and network reconfiguration in active distribution networks," *IET Generation, Transmission & Distribution*, vol. 10, no. 8, pp. 1938–1946, 2016.
- [20] R. A. Jabr, R. Singh, and B. C. Pal, "Minimum loss network reconfiguration using mixed-integer convex programming," *IEEE Trans. on Power systems*, vol. 27, no. 2, pp. 1106–1115, 2012.
- [21] M. Farivar, C. R. Clarke, S. H. Low, and K. M. Chandy, "Inverter var control for distribution systems with renewables," in *Proc. IEEE Int. Conf. on Smart Grid Communications*, 2011, pp. 457–462.
- [22] M. E. Baran and F. F. Wu, "Network reconfiguration in distribution systems for loss reduction and load balancing," *IEEE Trans. on Power delivery*, vol. 4, no. 2, pp. 1401–1407, 1989.

- [23] [Online]. Available: <http://www.tepco.co.jp/forecast/html/images/juyo-2014.csv>
- [24] Japan Meteorological Agency. [Online]. Available: <http://www.jma.go.jp/jma/indexe.html>



**Shunnosuke Ikeda** received his Bachelor of Engineering degree in the Department of System Design Engineering from Keio University in 2016. He is currently pursuing a Master of Engineering degree in Keio University. His research interests include distribution network planning, power system operation and optimization in power systems.



**Hiromitsu Ohmori** received Bachelor of Electrical Engineering and Ph.D. from Keio University, Japan in 1983, 1985 and 1988, respectively. From April 1988 he was the instructor of Department of Electrical Engineering, Keio University, Japan. From April 1991 he was the Assistant Professor of the same department. From April 1996 he was the Associate Professor of Department of System Design Engineering, Keio University. Currently he is working as Professor at the same department. His research interests are adaptive control, robust control, nonlinear control and their applications. He is member of IEEE, ISCIE, IEE, IEICE and EICA etc.